

Monte Carlo on a single sample

Nils Detering, Paul Eisenberg, Nicole Hufnagel

September 23, 2025

Abstract

In this paper, we consider a Monte Carlo simulation method (MinMC) that approximates prices and risk measures for a range Γ of model parameters at once. The simulation method that we study has recently gained popularity [HS20, FPP22, BDG24], and we provide a theoretical framework and convergence rates for it. In particular, we show that sample-based approximations to $\mathbb{E}_\theta[X]$, where θ denotes the model and \mathbb{E}_θ the expectation with respect to the distribution P_θ of the model θ , can be obtained across all $\theta \in \Gamma$ by minimizing a map $V : H \rightarrow \mathbb{R}$ with H a suitable function space. Minimization can be achieved easily by fitting a standard feedforward neural network with stochastic gradient descent. We show that MinMC, which uses only one sample for each model, significantly outperforms a traditional Monte Carlo method performed for multiple values of θ , which are subsequently interpolated. Our case study suggests that MinMC might serve as a new benchmark for parameter-dependent Monte Carlo simulations, which appear not only in quantitative finance but also in many other areas of scientific computing.

1 Introduction

We consider a set Γ of risk neutral models for pricing options, where (Γ, d_Γ) is a separable, metric space and \mathcal{B} its Borel- σ -algebra. Under a fixed model $\theta \in \Gamma$, we denote the price process defined on some measurable space (Ω, \mathcal{A}) by $(S_t^\theta)_{t \geq 0}$ and choose a payoff function p . Hence, the price of the European option with payoff function p in the model θ is

$$C(\theta) := \mathbb{E}[p(S_T^\theta)]. \quad (1)$$

When no analytic expression for the price $C(\theta)$ is available in the model θ , usually a Monte Carlo simulation is performed by simulating M i.i.d. samples

of $p(S_T^\theta)$ and calculating

$$C(\theta) = \lim_{M \rightarrow \infty} \frac{1}{M} \sum_{i=1}^M p(S_T^\theta(\omega_i)). \quad (2)$$

This methodology is widely adopted (see for instance [Gla04]), and according to the Central Limit Theorem (CLT), cf. [Pag18], the variance associated with the approximation error is $\text{Var}(p(S_T^\theta))/M$. In this context, we fix θ and undertake a Monte Carlo simulation for the selected model. When considering an alternative model, such as a slight modification of a parameter, M additional samples are required. For minor variations in θ , it is anticipated that the price will not change significantly. However, with the new full Monte Carlo simulation, the information derived from our prior samples remains completely unused. Our objective is to implement this approach more efficiently with a procedure that uses as little as one sample for each model θ but makes use of the continuity of the map $\theta \mapsto C(\theta)$. We derive convergence rates for the approximation error for this procedure across the entire set of models Γ . We emphasize that the problem of calculating $C(\theta)$ for all $\theta \in \Gamma$ is particularly important for applications. The parameters of models used at a derivative trading desk are frequently changing, often necessitating Monte Carlo simulations to be rerun whenever there is a change in the price of the underlying assets. In addition, for calibration of a model to the market or the calculation of Greeks, one needs option prices for a range of model specifications. Therefore, a procedure capable of directly calculating the entire function $C : \Gamma \rightarrow \mathbb{R}$ carries a substantial advantage. Moreover, our more general setup introduced below is suitable for most parameter-dependent Monte Carlo simulations. It therefore applies not only to option pricing, but also to many risk management tasks in the banking and insurance business where it is often important to calculate expectations for a range of different model parameters to access model risk (see, for example, [Con04, DP16, JS20, BC24, LQT24]).

For the approach to Monte Carlo simulation considered in this paper, we construct an extension $X : \Omega \times \Gamma \rightarrow \mathbb{R}$ for the payoff, where, for a given model $\theta \in \Gamma$, the distribution of $X(\cdot, \theta)$ is known (for example $X(\omega, \theta) := p(S_T^\theta(\omega))$ for the case of a European payoff mentioned above). Then, we specify a random variable Θ with distribution μ that characterizes the model. Let $h : \Gamma \rightarrow \mathbb{R}$ be a measurable function such that all expectations below are finite. Given the particular specification of Θ and the probability measure \mathbb{P} on $(\Gamma \times \Omega, \mathcal{B} \otimes \mathcal{A})$ described in Section 2, the following calculation holds:

$$\begin{aligned} V(h) &:= \mathbb{E}[|X - h(\Theta)|^2] = \int_{\Gamma} \mathbb{E}_{\theta}[|X - h(\theta)|^2] d\mu(\theta) \\ &= \int_{\Gamma} \mathbb{E}_{\theta}[X^2] - \mathbb{E}_{\theta}[X]^2 d\mu(\theta) + \int_{\Gamma} (\mathbb{E}_{\theta}[X]^2 - 2\mathbb{E}_{\theta}[X]h(\theta) + h(\theta)^2) d\mu(\theta) \quad (3) \\ &\stackrel{(1)}{=} \int_{\Gamma} \text{Var}_{\theta}[X] d\mu + \int_{\Gamma} (\mathbb{E}_{\theta}[X] - h(\theta))^2 d\mu(\theta), \end{aligned}$$

where Var_θ and \mathbb{E}_θ are such that $\mathbb{E}[X | \Theta] = (\mathbb{E}_\theta[X])|_{\theta=\Theta}$ and $\text{Var}[X | \Theta] = (\text{Var}_\theta[X])_{\theta=\Theta}$. We notice that only the second term in (3) actually depends on h . Thus, we can minimize the above expression $h \mapsto V(h)$ by choosing $h_0(\theta) = \mathbb{E}_\theta[X]$, which is the price of the option in the model θ . This is basically a random field extension (see, for instance [HS20, BBG⁺21]) of the well-known \mathcal{L}^2 approximation of expectation.

In summary, the aim is to find a function $h_0 : \Gamma \rightarrow \mathbb{R}$ satisfying

$$h_0(\Theta) = \mathbb{E}[X | \Theta]$$

using a numerical method when the laws of Θ and the conditional law P_θ^X of X given $\Theta = \theta$ are known but there are no analytic formulas available for calculating the conditional expectation. As in (2), this could be achieved numerically via choosing N positions $\Theta_1, \dots, \Theta_N$ and approximating $h(\Theta_i)$ with M Monte Carlo simulations each. Based on the previous considerations, however, we proceed differently. We begin by approximating the function $h \mapsto V(h)$ based on N i.i.d. observations of (X, Θ) . Afterwards, we compute the minimum h_N of this approximation and finally prove that h_N converges to the minimum h_0 of V for $N \rightarrow \infty$, provided a ridge term is added that prevents overfitting. The ridge term needs to converge to 0, but at a rate that is not too fast. In summary, we choose a sample-dependent minimization and show that it converges to the minimum of V . The minimization step can, for example, be performed using a stochastic gradient descent algorithm that determines optimal weights for a neural network that approximates h_N . In the following, we often refer to this method as MinMC. For each fixed model θ , in contrast to a classical Monte Carlo simulation, with the baseline MinMC at most one sample is actually generated ($M = 1$). This is possible due to an explicit use of the continuity properties of the function $h_0 : \Gamma \rightarrow \mathbb{R}$. Although our results cover the extreme case $M = 1$, we show that it is often advisable to choose M a bit larger, where in our case study, the optimal choice for M ranges between 1 and 100 depending on the problem. Within our case study, we demonstrate that determining $\mathbb{E}[X | \Theta]$ as the minimizer of a sample-based approximation of the mapping $h \mapsto V(h)$ significantly surpasses the performance of traditional Monte Carlo simulations conducted across multiple values of θ , which are subsequently interpolated. Although our case studies focus primarily on option pricing, the methodology is general and applicable across various domains in scientific computing that involve Monte Carlo simulations which depend continuously on a parameter.

To prove our convergence results, we understand the function u_0 as an element in a reproducing kernel Hilbert space H . This allows us to rewrite the sample-based approximation of V plus a ridge term as a convex quadratic operator whose minimizer can be shown to be unique and explicitly expressed. Resorting to a series of operator-theoretic results allows us to obtain our convergence rates.

1.1 Literature review

The methodology for computing $\mathbb{E}[X | \Theta]$ in the context of derivative pricing via the minimization of a functional analogous to $h \mapsto V(h)$ in a class of neural networks was initially proposed in [HS20] and compared with more classical regression techniques in [FPP22]. In [HS20] a heuristic convergence argument is provided, but without convergence rates. In [BBG⁺21] a similar method is used for solving the Kolmogorov partial differential equation using deep learning based on the Feynman-Kac formula. Notably, [BBG⁺21] demonstrates that the minimizer coincides with the solution of the targeted PDE, which is subsequently approximated using neural networks. In [BDG24] continuity results for the maps $h \mapsto V(h)$ and $\theta \mapsto h(\theta)$ have been established to adapt the method for flow forward pricing in commodity markets where the situation is further complicated by the infinite-dimensional nature of Γ . However, none of these papers addresses the question of an approximation with finitely many samples and its related convergence rates. This paper closes this gap in the literature by conducting a rigorous analysis and deriving convergence rates of MinMC within a broad framework, highlighting its applicability across diverse scenarios but with a particular focus on option pricing. Our case study suggests that MinMC might serve as a new benchmark for parameter-dependent Monte Carlo simulations that appear not only in quantitative finance but in many areas of scientific computing.

From a technical perspective, our work has some connection to the field of functional regression where the goal is to infer an unknown function $f : \mathbb{R}^d \rightarrow \mathbb{R}$. In this context, $f(\theta)$ is approximated based on samples $\{(\Theta_i, X_i)\}_{i=1}^n$, where Θ_i represents an input and X_i is the observed response generated by the error model

$$X_i = f(\Theta_i) + \varepsilon_i, \tag{4}$$

where ε_i is a noise term with $\mathbb{E}[\varepsilon_i] = 0$ and $\text{Var}(\varepsilon_i) = \sigma^2$. The most common way for estimating $f : \Gamma \rightarrow \mathbb{R}$ is by means of *Parametric regression* (see, for example [DS98, MPV12]), where one assumes a fixed functional form (e.g., linear for linear regression) which has the advantage that the number of parameters to be estimated is usually low. However, it comes at the cost of a restricted shape for f . An alternative is *nonparametric estimation* (e.g., kernel regression, splines) where no specific structure is assumed (see [Sto77, Sto80, HM85] and the comprehensive manuscript [Här90]) and therefore more general functions f can be estimated. Non-parametric regression techniques can be used for estimating conditional expectation when f is given by $f(\Theta) = \mathbb{E}[X | \Theta]$. More closely related to our approach is reproducing kernel Hilbert space (RKHS) regression. Kernel Hilbert space regression is regarded as a non-parametric regression approach wherein the selected RKHS imposes constraints on the regression function. This has recently been used for estimating the yield curve [FPY22], for statistical estimation of conditional expectation and variance from time-series in [FS25] and for uniform function estimation in [DP21]. Qualitatively, there is a key difference between the regression problem and MinMC.

In fact, for MinMC, the conditional distribution of X given Θ_i , is known and one can sample from it. The goal is then an efficient numerical technique to approximate $h_0(\Theta) = \mathbb{E}[X | \Theta]$. The reproducing kernel Hilbert space approach comes in handy for MinMC as it imposes only minimal structure on the function h_0 and its approximating functions, and therefore in particular allows for approximations with neural networks and the stochastic gradient descent optimizer.

Our paper is organized as follows. In Section 2, we summarize our main mathematical result Theorem 2.2 and provide some specific frameworks with examples. In Section 3, we provide a detailed proof of the main result as well as several helpful lemmas. Section 4 contains two case studies. The first highlights our method on the Black-Scholes model where simple benchmarking is possible. The second is applied to the Heston model where no closed-form price formula is known. Additional technical results can be found in the appendix.

2 Main results

We consider a random variable $X : \Omega \rightarrow \mathbb{R}$, which specifies the payoff. Let P be a probability transition kernel from Γ to Ω , that is, $P : \Gamma \times \mathcal{A} \rightarrow [0, 1]$ with

- (i) P_θ is a probability measure on (Ω, \mathcal{A}) for any $\theta \in \Gamma$ and
- (ii) $\theta \mapsto P_\theta(A)$ is measurable for any $A \in \mathcal{A}$.

For a probability measure μ on (Γ, \mathcal{B}) we define the probability measure \mathbb{P} on $(\Gamma \times \Omega, \mathcal{B} \otimes \mathcal{A})$ via

$$\mathbb{P}(B \times A) := \int_B P_\theta(A) \mu(d\theta), \quad B \in \mathcal{B}, A \in \mathcal{A}.$$

We introduce on $(\Gamma \times \Omega, \mathcal{B} \otimes \mathcal{A})$ the random variable $\Theta(\theta, \omega) := \theta$, with $\theta \in \Gamma$ and $\omega \in \Omega$, to describe the distribution of the possible models. We observe that its law under \mathbb{P} is given by $\mathbb{P}^\Theta = \mu$. Extending the random variable X to the product space $\Gamma \times \Omega$ by $X(\theta, \omega) := X(\omega)$, we find that

$$\mathbb{E}[X | \Theta] = (\mathbb{E}_\theta[X])|_{\theta=\Theta}$$

if $X \geq 0$ or $\mathbb{E}[|X|] < \infty$ where \mathbb{E}_θ denotes expectation under P_θ and \mathbb{E} expectation under \mathbb{P} . We denote the corresponding \mathcal{L}^p -spaces by

$$\begin{aligned} \mathcal{L}^p(\mu) &:= \left\{ g : \Gamma \rightarrow \mathbb{R} \mid g \text{ measurable}, \|g\|_{\mathcal{L}^p(\mu)} := \left(\int_\Gamma |g(\theta)|^p d\mu(\theta) \right)^{\frac{1}{p}} < \infty \right\}, \\ \mathcal{L}^p(\mathbb{P}, A) &:= \left\{ g : \Gamma \times \Omega \rightarrow A \mid g \text{ measurable}, \|g\|_{\mathcal{L}^p(\mathbb{P}, A)} := \left(\mathbb{E}(|g|^p) \right)^{\frac{1}{p}} \right\}. \end{aligned}$$

For simplicity we omit the image space A in the case of real functions. In case $X \in \mathcal{L}^2(\mathbb{P})$, then by construction, it holds that $\text{Var}[X | \Theta] = (\text{Var}_\theta[X])_{\theta=\Theta}$ where Var_θ denotes the variance under P_θ . In this setting, the motivating calculations presented in (3) apply. Based on these considerations, our goal is to determine the argmin of V over a suitable function space.

First, we specify the function space. Let $H \subset C(\Gamma, \mathbb{R})$ be a Hilbert space such that the point evaluation in H is a continuous linear functional. We denote the scalar product of H by $\langle \cdot, \cdot \rangle$ and its norm by $\|\cdot\|$. Due to Riesz representation theorem [Rud91, Thm. 12.5], there exists a function $k : \Gamma \times \Gamma \rightarrow \mathbb{R}$ such that $k_t := k(t, \cdot) \in H$ and $\langle h, k_t \rangle = h(t)$ for $h \in H, t \in \Gamma$. In other words, H is a reproducing kernel Hilbert space, see [Jon15, SFL11].

In this section, we present our main results and provide examples for the space H . Consider the i.i.d. sequence $\{(X_n, \Theta_n)\}_{n \in \mathbb{N}}$ where (X_1, Θ_1) has the same law as (X, Θ) . We proceed under the following assumptions:

Assumptions 2.1.

(A1) The random variable $\theta \mapsto k(\theta, \theta)$ has finite second μ -moment:

$$\int_{\Gamma} (k(\theta, \theta))^2 \mu(d\theta) < \infty.$$

(A2) The support of μ is Γ :

$$\Gamma = \bigcap \{A \subseteq \Gamma : A \text{ closed, } \mu(A) = 1\}.$$

(A3) $X : \Gamma \times \Omega \rightarrow \mathbb{R}$ is a random variable which satisfies $\mathbb{E}[X^4] < \infty$.

(A4) There is $h_0 \in H$ such that

$$\mathbb{E}[X | \Theta] = h_0(\Theta).$$

(A1) guarantees $\mathbb{E}[h(\Theta)^4] < \infty$ for any function $h \in H$, see Theorem A.1. The support property (A2) of Θ yields that any two elements of H which are \mathbb{P}^Θ -a.s. equal are equal, see Theorem A.2.

We consider the quadratic functions $V : H \rightarrow \mathbb{R}$ and $V_N : H \rightarrow \mathcal{L}^2(\mathbb{P})$ given by

$$\begin{aligned} V(h) &= \mathbb{E}[(h(\Theta) - X)^2] \\ V_N(h) &:= \frac{1}{N} \sum_{i=1}^N (h(\Theta_i) - X_i)^2 \end{aligned}$$

for any $h \in H$. In addition, we introduce regularised versions that include a ridge term; for $\lambda > 0$ we define

$$V_\lambda(h) := V(h) + \lambda \|h\|^2, \quad V_{N,\lambda}(h) := V_N + \lambda \|h\|^2.$$

We note that the minimizer of V is the function h_0 , see (A4). According to our goal, we need to approximate h_0 from a sample $(X_1, \Theta_1), \dots, (X_N, \Theta_N)$. For a given sample $(X_1, \Theta_1), \dots, (X_N, \Theta_N)$ the penalty $V_{N,\lambda}$ is explicitly specified via

$$V_{N,\lambda}(h) = \frac{1}{N} \sum_{i=1}^N (h(\Theta_i) - X_i)^2 + \lambda \|h\|^2.$$

Optimizing this penalty can be achieved by large enough neural network, cf. universal approximation theorem in [HSW89]. The obtained network g satisfies $g \approx h_{N,\lambda}$ and with the choice of λ in Theorem 2.2 below, we can then ensure that $g \approx h_0$.

The proof of the following theorem, which establishes a bound on the convergence rate of MinMC, is given in Section 3.

Theorem 2.2. The minimizer $h_{N,\lambda}$ of $V_{N,\lambda}$ exists for any $N \in \mathbb{N}, \lambda > 0$. There is a constant $C > 0$ such that

$$\mathbb{E}[\|h_{N,\lambda_N} - h_0\|_{\mathcal{L}^2(\mu)}] \leq C \max \left\{ \lambda_N^{-2} N^{-\frac{1}{2}}, \sqrt{\lambda_N} \right\}, \quad N \in \mathbb{N} \quad (5)$$

for any $N \in \mathbb{N}, \lambda > 0$.

Remark 2.3. For the application of Theorem 2.2 we assume that $\lambda_N \rightarrow 0$ and $\lambda_N N^{\frac{1}{4}} \rightarrow \infty$ to ensure $\lim_{n \rightarrow \infty} \mathbb{E}[\|h_{N,\lambda_N} - h_0\|_{\mathcal{L}^2(\mu)}] = 0$. Since $\lambda_N^{-2} N^{-\frac{1}{2}}$ decreases monotonically and $\sqrt{\lambda_N}$ increases monotonically in λ_N , the optimal rate in (5) is obtained when $\lambda_N^{-2} N^{-\frac{1}{2}} = \sqrt{\lambda_N}$. Hence, the optimal rate for the right hand side is $N^{-\frac{1}{10}}$ when $\lambda_N = N^{-\frac{1}{5}}$. Compared to the classical Monte Carlo rate of $N^{-1/2}$, this rate may not look impressive. However, it should be noted that the approximation is applied throughout the model class Γ instead of only for one model $\theta \in \Gamma$. Moreover, the rate is independent of the dimension of Γ . Our case study in Section 4 shows a superior performance of MinMC even when compared on a finite deterministic subset $\theta_1, \dots, \theta_K$ with a classical Monte Carlo simulations performed exactly for the models $\theta_1, \dots, \theta_K$. Like all Monte Carlo methods, a larger sample yields a better theoretical approximation. In addition, a larger network and longer training should give a better approximation g of the approximator $h_{N,\lambda}$.

For a neural network g with $g \approx h_{N,\lambda}$, it is important to also understand the mse-loss of the network. The next proposition shows that the mse-loss is approximately equal to the expected conditional variance of X . This is despite the fact that we already know that $h_{N,\lambda} \rightarrow h_0$ for $N \rightarrow \infty$ and $\lambda \rightarrow 0$.

The proof of the following proposition is given in Section 3.

Proposition 2.4. The minimizer $h_{N,\lambda}$ of $V_{N,\lambda}$ exists for any $N \in \mathbb{N}, \lambda > 0$. For $\lambda_N \rightarrow 0$ and $\lambda_N N^{\frac{1}{4}} \rightarrow \infty$ the following convergence holds:

$$\lim_{N \rightarrow \infty} \frac{1}{N} \sum_{i=1}^N (h_{N,\lambda_N}(\Theta_i) - X_i)^2 = \mathbb{E}[\text{Var}(X | \Theta)]$$

as $N \rightarrow \infty$ in $\mathcal{L}^1(\mathbb{P})$.

In the following, we provide examples that align with our framework. In each case, we begin by introducing our set of models Γ , a subset of \mathbb{R}^n , along with the corresponding Hilbert space H and the function k that satisfies all the required properties. Then, we present an example for the payoff X that satisfies (A3) and (A4).

First, we focus on translation invariant k , that is, there exists a function ψ such that $k(x, y) = \psi(x - y)$, see [SFL11, p. 2393].

Lemma 2.5. Let $\Gamma \subset \mathbb{R}^n$. If there exists a continuous, positive-definite and symmetric function $\psi : \mathbb{R}^n \rightarrow \mathbb{R}$ such that $k(x, y) = \psi(x - y)$ then k satisfies (A1) for any measure μ on Γ . Furthermore, there is a Hilbert space

$$H \subseteq C(\Gamma, \mathbb{R})$$

with some scalar product such that

- (i) $k_x \in H$ for any $x \in \Gamma$ and
- (ii) $\langle f, k_x \rangle = f(x)$ for any $x \in H$.

Proof. We have $k(\theta, \theta) = \psi(0)$ which guarantees (A1) for any measure μ on Γ , that is, finite second μ -moment. The function k receives the properties continuous, positive-definite and symmetric from ψ . Hence, the existence of a Hilbert space satisfying (i) and (ii) follows by the Moore-Aronszajn Theorem [Aro50, p. 344]. \square

Example 2.6. We consider the Hilbert space

$$\begin{aligned} H &:= \{f : [0, 1] \rightarrow \mathbb{R} \mid f \text{ absolutely continuous with } f' \in \mathcal{L}^2(\mathcal{U}([0, 1]))\} \\ &\subseteq C([0, 1], \mathbb{R}) \end{aligned}$$

with scalar product

$$\langle f, g \rangle := \frac{1}{2}(f(1) + f(0))(g(1) + g(0)) + \frac{1}{2} \int_0^1 f'(x)g'(x)dx.$$

Here, $\Gamma := [0, 1]$ specifies the models for pricing options with a continuous uniform distribution $\mu := \mathcal{U}([0, 1])$. For $x \in [0, 1]$ the function $k_x : [0, 1] \rightarrow \mathbb{R}$ given via $k_x(y) := 1 - |x - y|$ fulfills $k_x \in H$ and

$$\langle k_x, f \rangle = f(x)$$

for $f \in H$. Consequently,

$$k(x, y) := k_x(y) = 1 - |x - y|$$

satisfies the desired properties.

Assumption (A1) holds by Theorem 2.5 since k is a translation-invariant function. The support property (A2) is valid due to the choice of μ . Apparently, we can choose a different μ such that (A2) remains fulfilled. Furthermore, we ensure $\mathbb{E}[X^4] \leq C < \infty$ and that $h_0(\theta) = \mathbb{E}_\theta[X]$ is Lipschitz continuous which implies (A3) and (A4).

A classic and well-known example that fits into this framework is the Black-Scholes model with volatility ranging for example between 10% – 20%, see [BS73]. We select the volatility as $(1 + \theta) \cdot 0.1$ for $\theta \in [0, 1]$. In this case, the underlying asset price follows a geometric Brownian motion with volatility θ , initial price $x > 0$, and a risk-free interest rate $r > 0$. The payoff of a European call option is then given by:

$$X := (xe^{Z_T} - K)_+ := \max \{ xe^{Z_T} - K, 0 \},$$

where $K > 0$ is the strike price, $T > 0$ is the maturity, and

$$Z_T \sim \mathcal{N} \left(-\frac{1}{200}(1 + \theta)^2 T, \frac{(1 + \theta)^2}{100} T \right) \text{ under } P_\theta.$$

Since the norm of X is bounded by a geometric Brownian motion, it immediately follows $\mathbb{E}[X^4] < \infty$. Here, the price formula of the option is known, [BS73, Eq. (13)],

$$\begin{aligned} h_0(\Theta) &= \mathbb{E}[X | \Theta] \\ &= x\Phi \left(d_1 \left(\frac{1 + \Theta}{10} \right) \right) - Ke^{-rT}\Phi \left(d_1 \left(\frac{1 + \Theta}{10} \right) - \frac{(1 + \Theta)\sqrt{T}}{10} \right) \end{aligned}$$

with Φ the cumulative distribution function of $\mathcal{N}(0, 1)$ and

$$d_1(\sigma) := \frac{\ln \left(\frac{x}{K} \right) + (r + \frac{1}{2}\sigma^2)T}{\sigma\sqrt{T-t}}.$$

The function h_0' is continuous and its absolute value is bounded on $[0, 1]$, hence h_0 is Lipschitz continuous.

Obviously, this setting works for any volatility interval $[a, b] \subset [0, \infty)$ by choosing the volatility $a + \theta(b - a)$ for $\theta \in [0, 1]$. In addition, we can choose a more general European or even path dependent payoff.

Example 2.7. We consider the Sobolov space

$$H^\alpha(\mathbb{R}^n) := \left\{ f \in \mathcal{L}^2(\lambda^n) \mid \int_{\mathbb{R}^n} (1 + |x|^\alpha) |\widehat{f}(x)|^2 d\lambda^n(x) < \infty \right\}$$

with scalar product

$$\langle f, g \rangle_\alpha := (2\pi)^{-\frac{n}{2}} \int_{\mathbb{R}^n} (1 + |x|^\alpha) \widehat{f}(x) \overline{\widehat{g}(x)} d\lambda^n(x)$$

where \widehat{f} represents the Fourier transform for integrable f , that is,

$$\widehat{f}(x) := (2\pi)^{-\frac{n}{2}} \int_{\mathbb{R}^n} f(y) e^{i\langle x, y \rangle} d\lambda^n(y)$$

and λ^n the Lebesgue measure on \mathbb{R}^n .

The function $k_x : \mathbb{R}^n \rightarrow \mathbb{R}$ is given via

$$\widehat{k}_x(u) := \frac{e^{i\langle u, x \rangle}}{1 + |u|^\alpha}.$$

For $\alpha > \frac{n}{2}$, $x \in \mathbb{R}^n$ it holds that $\widehat{k}_x \in \mathcal{L}^2(\lambda^n)$ and one finds $k_x \in H_\alpha$ and for $f \in H_\alpha$ that

$$\langle f, k_x \rangle_\alpha = f(x).$$

Due to Sobolev embedding theorem [AF03, Ch. 6], H^α contains $C^\alpha(\mathbb{R}^n, \mathbb{R})$ with compact support for $\alpha \geq \frac{n}{2}$.

If $n = 1$ and $\alpha = 2$, then we find

$$k_x(y) = ce^{-|x-y|}$$

for some constant $c > 0$ because $u \mapsto \frac{1}{\pi(1+|u|^2)}$ is the density of the Cauchy distribution.

The function k is again translation-invariant, hence (A1) holds, see Theorem 2.5. We then have to choose a measure μ with support \mathbb{R}^n , i.e., (A2) and a random variable X such that (A3) and (A4) apply.

Example 2.8. The space presented in Filipović [Fil01] is another convenient RKHS. For a continuously differentiable and non-decreasing function $w : [0, \infty) \rightarrow [1, \infty)$ with $w(0) = 1$. Let now H be the set of all absolutely continuous functions $f : [0, \infty) \rightarrow \mathbb{R}$ for which

$$\int_0^\infty (f'(x))^2 w(x) dx < \infty. \quad (6)$$

With the inner product defined by

$$\langle f, g \rangle := f(0)g(0) + \int_0^\infty f'(x)g'(x)w(x) dx, \quad \text{for } f, g \in H_w,$$

and $\|f\|^2 := \langle f, f \rangle$, this space is a separable Hilbert space with $H_w \subset C([0, \infty), \mathbb{R})$, see [Fil01, Theorem 5.1.1]. Moreover, $f(x) = \langle f, k_x \rangle$ and $k_x \in H_w$ with k_x defined by

$$k(x, y) := k_x(y) := 1 + \int_0^{y \wedge x} (w(z))^{-1} dz.$$

In this setting, we have $\Gamma := [0, \infty)$ with some probability measure μ with support Γ , i.e., (A2). If w^{-1} is chosen to be integrable, then $k_x(y) \leq C < \infty$

and (A1) is true. Finally, we choose a payoff X such that (A3) and (A4) are valid.

Similar to Example 2.6 the Black-Scholes model with volatility $\theta \in [0, \infty)$ fits into this setting. Using the same notation, the payoff is

$$X := (xe^{Z_T} - K)_+$$

with

$$Z_T \sim \mathcal{N}\left(-\frac{1}{2}\theta^2 T, \theta^2 T\right) \text{ under } P_\theta$$

and corresponding price formula

$$h_0(\Theta) = \mathbb{E}[X | \Theta] = x\Phi(d_1(\Theta)) - Ke^{-rT}\Phi(d_1(\Theta) - \Theta\sqrt{T}).$$

For $w(x) := e^x$ we have $h_0 \in H_w$, and $\mathbb{E}[X^4] < \infty$ as X is bounded by a geometric Brownian motion. For example, choosing μ as the exponential distribution, this example fulfills all assumptions.

Example 2.9. A feature map is any function

$$\phi : \Gamma \rightarrow H,$$

where Γ is some set and H any Hilbert space.

In the following, we use the specific Hilbert space H given by $H = \mathcal{L}^2(\mathbb{R}^d, R)$ for some chosen probability measure R . For $x \in \Gamma$ we write ϕ_x for the image of x under ϕ and treat it as a random variable, that is, we consider $\mathbb{E}_R[XY]$ for the scalar product of $X, Y \in H$. Let $\sigma : \mathbb{R} \rightarrow \mathbb{R}$ be measurable and bounded. We define

$$\phi_x := \sigma(x + \cdot) \in H$$

for any $x \in \mathbb{R}^d$ where σ is applied component-wise. Then, ϕ is a feature map. Recall that $k(x, y) := \mathbb{E}_R[\phi_x \phi_y]$ for $x, y \in \Gamma$ defines a kernel on Γ , cf. [Aro50]. For $X \in H$ we define $f_X : \Gamma \rightarrow \mathbb{R}$, $x \mapsto \mathbb{E}_R[X \phi_x]$ and note that

$$\Phi : H \rightarrow H_k, X \mapsto f_X$$

is a surjective, continuous, linear map from H to H_k .

Observe that

$$|f|_{H_k}^2 = \inf_{X \in H, f_X = f} \mathbb{E}_R[X^2].$$

Further, we consider a generic quadratic function on H_k

$$q(f) := \langle Qf, f \rangle_{H_k} - 2\langle a, f \rangle_{H_k} + c$$

where Q is positive-semidefinite on H_k , $a \in H_k$ and $c \in \mathbb{R}$, and assume that f_0 is a minimizer for q .

We define the quadratic function

$$\bar{q}(X) := q(\Phi(X)), \quad X \in H.$$

Note that \bar{q} has a minimizer and any minimizer X_0 of \bar{q} satisfies $\Phi(X_0) = f_0$. This allows to pull the minimization problem of q in H_k to \bar{q} in H . The latter has a known norm which might be easier implemented in some cases.

Additionally, if the function $f \mapsto q(f) + \lambda \|f\|_{H_k}^\alpha$ is to be minimized over f for some fixed $\alpha \geq 1$, then the unique minimizer X_0 of

$$X \mapsto \bar{q}(X) + \lambda \|X\|_H^\alpha$$

satisfies that $\Phi(X_0)$ is a minimizer of $f \mapsto q(f) + \lambda \|f\|_{H_k}^\alpha$ due to the norm representation.

Note though, kernel ridge regression can also be implemented without knowledge of the norm on the RKHS but relies on the (numerical) solution f_0 to $(Q + \lambda)f_0 = a$ on the finite dimensional subspace generated by k_{x_1}, \dots, k_{x_N} where $x_1, \dots, x_N \in \Gamma$ are the observation points, see [SHS01, Theorem 1] for details. If the number of observations N is high, this is a technical problem on its own.

An approximation of kernel ridge regression via neural networks and gradient descent on the other hand requires the implementation of the norm of the given space for the penalty term. Here, it is useful to use a generic Hilbert space like a standard \mathcal{L}^2 -space where many known techniques are available for implementation of the norm. We shall make use of this observation in our case study.

In the above setting of a feature map with $H = \mathcal{L}^2(\mathbb{R}^d, R)$ we now consider a Heston model for the stock price:

$$\begin{aligned} dS_t &= \mu S_t dt + \sqrt{v_t} S_t dW_t^S, \\ dv_t &= \kappa(\theta - v_t)dt + \sigma \sqrt{v_t} dW_t^v, \\ dW_t^S dW_t^v &= \rho dt, \end{aligned}$$

where S_t is the stock price, and $\sqrt{v_t}$ the instantaneous volatility. The parameter κ determines the mean reversion speed to the long term variance θ , σ the volatility of the volatility (vol of vol), and ρ the constant correlation between the two Brownian motions W^S and W^v . In our case study in Section 4, we fix a payoff function and then aim to learn the map $(\kappa, \theta, \sigma, \rho) \mapsto P_{\kappa, \theta, \sigma, \rho}$, where $P_{\kappa, \theta, \sigma, \rho}$ is the price of the payoff under the Heston model with the parameters $\kappa, \theta, \sigma, \rho$.

3 Proofs of the main results

As a tool, we introduced a real reproducing kernel Hilbert space (RKHS). For a linear operator $T \in L(H)$ and $\lambda \in \mathbb{R}$ we understand by $T + \lambda$ the bounded

operator with $(T + \lambda)h := Th + \lambda h$. For $h \in H$ we define the operator $h \otimes h \in L(H)$ via

$$(h \otimes h)f := h\langle h, f \rangle, \quad f \in H.$$

We rewrite the quadratic functions V and V_N in terms of operator theory and the kernel k . Hence, we make the specifications $Q_N := \frac{1}{N} \sum_{i=1}^N k_{\Theta_i} \otimes k_{\Theta_i}$, $Q := \mathbb{E}[Q_1]$, $a_N := \frac{1}{N} \sum_{i=1}^N X_i k_{\Theta_i}$ and $a := \mathbb{E}[a_1]$. Thus,

$$\begin{aligned} V(h) &= \mathbb{E}[(h(\Theta) - X)^2] \\ &= \langle Qh, h \rangle - 2\langle a, h \rangle + \mathbb{E}[X^2] \\ V_N(h) &= \frac{1}{N} \sum_{i=1}^N (h(\Theta_i) - X_i)^2 \\ &= \langle Q_N h, h \rangle - 2\langle a_N, h \rangle + \frac{1}{N} \sum_{i=1}^N X_i^2. \end{aligned}$$

Due to Theorem A.8 we find that $Q \in L(H)$ and $Q_N \in \mathcal{L}^2(\mathbb{P}, L(H))$ are positive semidefinite operators on H which are trace-class and Hilbert Schmidt. Observe that, $a \in H$ and $a_N \in \mathcal{L}^2(\mathbb{P}, H)$. In the previous section, we introduced a regularized version by adding a small ridge term $\lambda\|h\|$. Using the operator representation of V , we now show that the minimum of the regularized version remains approximately the same for small λ .

Proposition 3.1. The unique minimizer of V is h_0 . Moreover, the minimizer h_λ for V_λ exists for $\lambda > 0$ and we have

$$\lim_{\lambda > 0, \lambda \rightarrow 0} h_\lambda = h_0.$$

Proof. We observe

$$\nabla V(h) = 2(Qh - a) = 2\mathbb{E}[k_\Theta(h(\Theta) - X)], \quad h \in H.$$

Conditioning on Θ implies

$$\nabla V(h_0) = \mathbf{0}.$$

Let $\tilde{h}_0 \in H$ be a minimizer for V . Then, we have

$$\mathbf{0} = \nabla V(\tilde{h}_0) = 2\mathbb{E}[k_\Theta(\tilde{h}_0(\Theta) - X)] = 2\mathbb{E}[k_\Theta(\tilde{h}_0(\Theta) - h_0(\Theta))]$$

where the last equality is obtained via conditioning on Θ . Consequently, we derive

$$0 = \langle \tilde{h}_0 - h_0, \nabla V(\tilde{h}_0) \rangle = 2\mathbb{E}[(\tilde{h}_0(\Theta) - h_0(\Theta))^2]$$

and thus $\tilde{h}_0 = h_0$ \mathbb{P}^Θ -a.s. Theorem A.2 yields $\tilde{h}_0 = h_0$. Due to Theorem A.8 Q has a trivial kernel. Theorem A.11 implies $h_\lambda \rightarrow h_0$ as $\lambda \rightarrow 0$. \square

To prove the main result, Theorem 2.2, we first need a few auxiliary statements, such as the following Monte Carlo bounds:

Lemma 3.2. For every $N \in \mathbb{N}$ we have

$$\begin{aligned}\mathbb{E}[\|a_N - a\|^2] &= \frac{\mathbb{E}[\|a_1 - a\|^2]}{N}, \\ \mathbb{E}[\|Q_N - Q\|_{HS}^2] &= \frac{\mathbb{E}[\|Q_1 - Q\|_{HS}^2]}{N}.\end{aligned}$$

Proof. The statement follows from Theorem B.1 and Theorem B.2. \square

Next, we show that the ridge regression V_λ can be solved approximately by the random ridge regression $V_{N,\lambda}$ and quantify the $\mathcal{L}^1(\mathbb{P}, H)$ error.

Proposition 3.3. Let $\lambda \in (0, 1]$. The minimizer $h_{N,\lambda} \in \mathcal{L}^2(\mathbb{P}, H)$ of the random quadratic function $V_{N,\lambda}$ exists and there is a constant $C > 0$ (not depending on N or λ) such that

$$\mathbb{E}[\|h_{N,\lambda} - h_\lambda\|] \leq \frac{C}{\lambda^2 \sqrt{N}}.$$

Proof. Lemma A.5 yields existence of the minimizer and

$$\begin{aligned}h_\lambda &= (Q + \lambda)^{-1}a, \\ h_{N,\lambda} &= (Q_N + \lambda)^{-1}a_N.\end{aligned}$$

Using Theorem A.6 we obtain

$$\|(Q_N + \lambda)^{-1} - (Q + \lambda)^{-1}\|_{op} \leq \frac{\|Q_N - Q\|_{op}}{\lambda^2}.$$

Thus, we find

$$\begin{aligned}\|h_{N,\lambda} - h_\lambda\| &\leq \|((Q_N + \lambda)^{-1} - (Q + \lambda)^{-1})a_N\| + \|(Q + \lambda)^{-1}(a_N - a)\| \\ &\leq \|((Q_N + \lambda)^{-1} - (Q + \lambda)^{-1})\|_{op} \|a_N\| + \|(Q + \lambda)^{-1}\|_{op} \|a_N - a\| \\ &\leq \frac{\|Q_N - Q\|_{op}}{\lambda^2} \|a_N\| + \frac{\|a_N - a\|}{\lambda},\end{aligned}$$

where we used Theorems A.3 and A.6 for the last inequality. Using expectation and the Cauchy-Schwarz inequality yields

$$\mathbb{E}[\|h_{N,\lambda} - h_\lambda\|] \leq \frac{1}{\lambda^2} \sqrt{\mathbb{E}[\|Q_N - Q\|_{op}^2]} \sqrt{\mathbb{E}[\|a_N\|^2]} + \frac{\mathbb{E}[\|a_N - a\|]}{\lambda}.$$

Exploiting the inequality $\|\mathcal{T}\|_{op} \leq \|T\|_{HS}$ which holds for any symmetric operator $T \in L(H)$ and Theorem 3.2 we derive

$$\mathbb{E}[\|h_{N,\lambda} - h_\lambda\|] \leq \frac{\sqrt{\mathbb{E}[\|Q_1 - Q\|_{HS}^2]}}{\sqrt{N} \lambda^2} \sqrt{\mathbb{E}[\|a_N\|^2]} + \frac{\sqrt{\mathbb{E}[\|a_1 - a\|^2]}}{\sqrt{N} \lambda}.$$

Since $\sqrt{\mathbb{E}[\|\cdot\|^2]}$ is a norm and due to Theorem 3.2 we have

$$\sqrt{\mathbb{E}[\|a_N\|^2]} \leq \sqrt{\mathbb{E}[\|a_N - a\|^2]} + \|a\| = \frac{\sqrt{\mathbb{E}[\|a_1 - a\|^2]}}{\sqrt{N}} + \|a\|.$$

Choosing

$$C := \sqrt{\mathbb{E}[\|Q_1 - Q\|_{HS}^2]} \left(\sqrt{\mathbb{E}[\|a_1 - a\|^2]} + \|a\| \right) + \sqrt{\mathbb{E}[\|a_1 - a\|^2]}$$

yields the claim. \square

Combining the previous results, we now prove the main result Theorem 2.2.

Proof of Theorem 2.2. Let $N \in \mathbb{N}$ and $\tilde{C} > 0$ be the constant from Proposition 3.3. Proposition A.11 yields $\|h_{\lambda_N} - h_0\|_{\mathcal{L}^2(\mu)} \leq \sqrt{\lambda_N} \|h_0\|/2$. Additionally using $\|h\|_{\mathcal{L}^2(\mu)} = (\langle Qh, h \rangle)^{1/2} \leq \|Q\|_{\text{op}}^{1/2} \|h\|$, we conclude

$$\begin{aligned} \mathbb{E}[\|h_{N,\lambda_N} - h_0\|_{\mathcal{L}^2(\mu)}] &\leq \mathbb{E}[\|h_{N,\lambda_N} - h_{\lambda_N}\|_{\mathcal{L}^2(\mu)}] + \|h_{\lambda_N} - h_0\|_{\mathcal{L}^2(\mu)} \\ &\leq \frac{\tilde{C} \|Q\|_{\text{op}}^{1/2}}{\lambda_N^2 \sqrt{N}} + \frac{\sqrt{\lambda_N} \|h_0\|}{2} \\ &\leq \left(\tilde{C} \|Q\|_{\text{op}}^{1/2} + \frac{\|h_0\|}{2} \right) \max \{ \lambda_N^{-2} N^{-\frac{1}{2}}, \sqrt{\lambda_N} \} \end{aligned}$$

as required. \square

Proof of Theorem 2.4. Lemma A.5 yields existence of the minimizer and

$$\begin{aligned} h_{N,\lambda} &= (Q_N + \lambda)^{-1} a_N, \\ V_N(h_{N,\lambda}) &= \frac{1}{N} \sum_{i=1}^N X_i^2 - \langle a_N, h_{N,\lambda} \rangle. \end{aligned}$$

Combining $a_N \rightarrow a$ in $\mathcal{L}^2(\mathbb{P}, H)$ with (A3) implies $\frac{1}{N} \sum_{i=1}^N X_i^2 \rightarrow \mathbb{E}[X^2]$ in $\mathcal{L}^2(\mathbb{P})$, and hence we find

$$\lim_{N \rightarrow \infty} V_N(h_{N,\lambda_N}) = V(h_0)$$

in $\mathcal{L}^1(\mathbb{P})$. We also have

$$V(h_0) = \mathbb{E}[(h_0(\Theta) - X)^2] = \mathbb{E}[(X^2 - \mathbb{E}[X | \Theta]^2)] = \mathbb{E}[\text{Var}(X | \Theta)].$$

\square

4 Case study

In this section, we present a simulation study to verify the results for MinMC numerically. We focus here on a European call option with strike $K = 100$ and the initial value of the asset $x = 100$. To compute the argmin of $V_{N,\lambda}$, we use a neural network. For the training, we use the gradient-based optimization algorithm Adam with 50 epochs, a batch size of 32, and a learning rate of 0.0001. For the network structure, we used the hyperbolic tangent as the activation function, with two hidden layers, and 200 nodes in each layer.

First, we take a closer look at the Black-Scholes model with volatility 10% – 20%. In Example 2.6 we introduce a suitable theoretical setting for the MinMC framework. Recall that the volatility is $(1 + \theta) \cdot 0.1$ for $\theta \in [0, 1]$. Since the price formula is known, an approximation is not necessary, but it allows us to verify the accuracy of our approximation results.

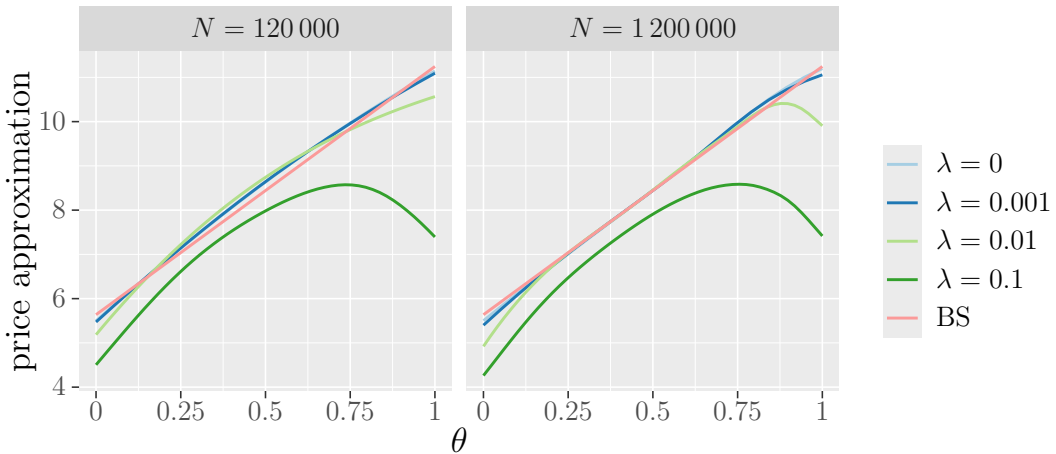


Figure 1: Model approximations for a European call option in the Black-Scholes model for different values of λ , but based on the same samples, compared to the true price (Black-Scholes formula).

In Figure 1 we visualize the price approximation for different values of λ based on the same samples $(X_1, \Theta_1), \dots, (X_N, \Theta_N)$ and the true price obtained using the Black-Scholes formula. A noticeable improvement is observed with decreasing λ . The results for $\lambda = 0$ and $\lambda = 0.001$ are nearly indistinguishable. Notably, $\lambda = 0$ produces excellent results, although we have not provided a formal proof in this case. For both values of N , the simulation for $\lambda = 0.1$ tends to significantly underestimate the price. Since the minimizer of $V_{N,\lambda}$ has a limit for every fixed $\lambda > 0$, see Theorem 3.3, the results suggest that this limiting behavior is effectively reached at $N = 120\,000$ for $\lambda = 0.1$. As mentioned in Theorem 2.3 we need $\lambda_N \rightarrow 0$ and $\lambda_N N^{\frac{1}{4}} \rightarrow \infty$, hence choosing $\lambda < N^{-\frac{1}{4}}$ seems reasonable. Here, $(120\,000)^{-\frac{1}{4}} \approx 0.0542$ justifies this behavior.

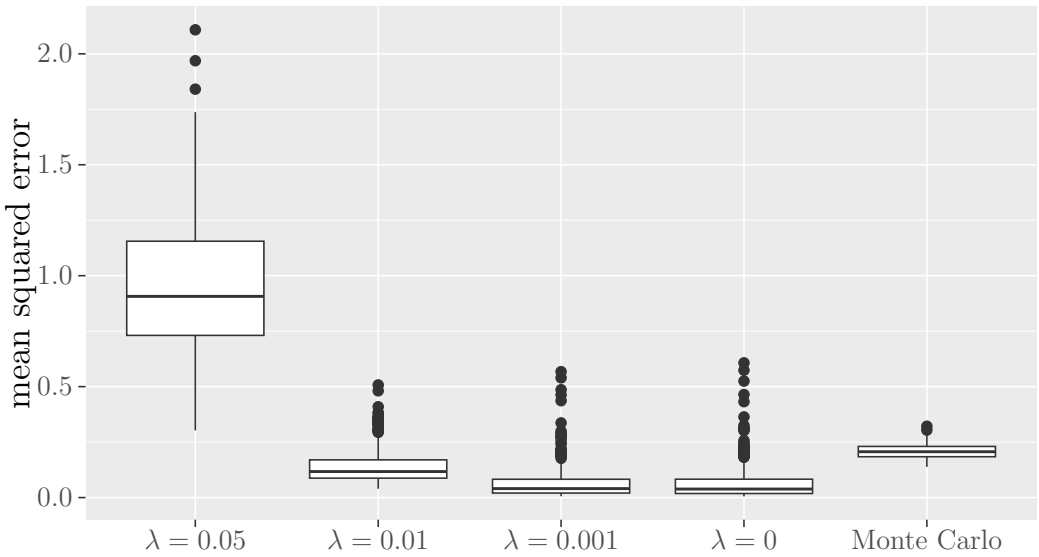


Figure 2: Mean squared error in the Black-Scholes model based on 500 simulation runs for $N = 100\,000$ compared to Monte Carlo simulations (each with 1 000 samples) for 100 θ values chosen equidistant in $[0, 1]$.

	median	25% quantile	75% quantile
$\lambda = 0.05$	0.9068	0.7310	1.1554
$\lambda = 0.01$	0.1173	0.0876	0.1700
$\lambda = 0.001$	0.0404	0.0204	0.0826
$\lambda = 0$	0.0385	0.0183	0.0828
Monte Carlo	0.2066	0.1842	0.2305

Table 1: Median, 25% and 75% quantiles of the mean squared error obtained from 500 repeated price approximations for various λ values and the Monte Carlo method. These values correspond to the boxplots shown in Figure 2.

Next, we fit the neural network 500 times using different training sets each time, compute the corresponding price approximations, and calculate the mean squared error for various values of λ . In comparison, we perform Monte Carlo simulations with 1 000 samples for 100 θ values, chosen equidistant in $[0, 1]$. In all cases, the mean squared error is calculated with respect to the Black-Scholes model on these equidistant values. For the MinMC neural network, we choose samples $N = 100 \cdot 1\,000$ to ensure that the simulation results are based on the same total number of random variables. The resulting boxplots are presented in Figure 2. The Monte Carlo simulation has the fewest outliers. This is not surprising since we calculate the mean squared errors on the 100 equidistant θ values and the Monte Carlo simulation is performed exactly for these values of θ . The boxplots show again an improvement with decreasing λ . Although no visible improvement can be observed when comparing $\lambda = 0.001$ and $\lambda = 0$ in Figure 2, the corresponding median and quantiles presented in

Table 1 indicate a slight improvement. MinMC provides better results than the Monte Carlo method for $\lambda \in \{0.01, 0.001, 0\}$.

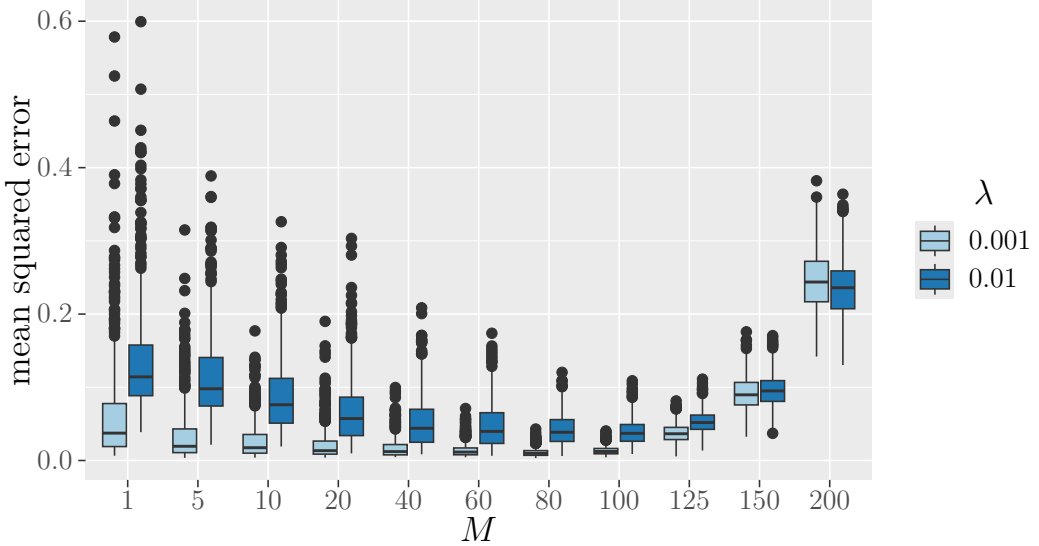


Figure 3: Mean squared error in the Black-Scholes model based on 500 simulation runs for $\lambda = 0.01$ and $\lambda = 0.001$ with fixed number of random variables $M \cdot N = 120\,000$. For fixed M the simulations are based on the same samples.

We now combine the MinMC setting with a Monte Carlo average to find the samples $(X_1, \Theta_1), \dots, (X_N, \Theta_N)$. For each model parameter Θ_i we sample M i.i.d. random variables $Y_{i,1}, \dots, Y_{i,M}$ from this model and define the average

$$X_i := \frac{1}{M} \sum_{j=1}^M Y_{i,j}. \quad (7)$$

This results in an i.i.d. sequence $(X_1, \Theta_1), \dots, (X_N, \Theta_N)$ which satisfies the MinMC assumptions. The conditional variance of the X_i , which appears in Proposition 2.4, is then lower as the conditional variance of $Y_{i,j}$. Increasing the number M allows to reduce the observed mse-error with increasing M . We fix the number of random variables $M \cdot N$ and calculate the mean squared error for different values of M . The results of 500 neural network fittings, each performed on a different training set, are visualized in Figure 3 for $\lambda = 0.01$ and $\lambda = 0.001$. Given that Θ_i is uniformly distributed over the interval $[0, 1]$, it can be assumed that some degree of averaging naturally occurs when considering a sufficiently large number of closely spaced values. In particular, MinMC performs well for $M = 1$. However, the boxplots clearly show that explicitly performing averaging yields improved results. The mean squared error initially decreases with increasing values of M , reaches an optimum in the range of $M = 60$ to $M = 125$, and subsequently increases as M continues to increase. The smallest median in Figure 3 is 0.0371 in the case $\lambda = 0.01$ for $M = 100$ and 0.0097 in the case $\lambda = 0.001$ for $M = 80$.

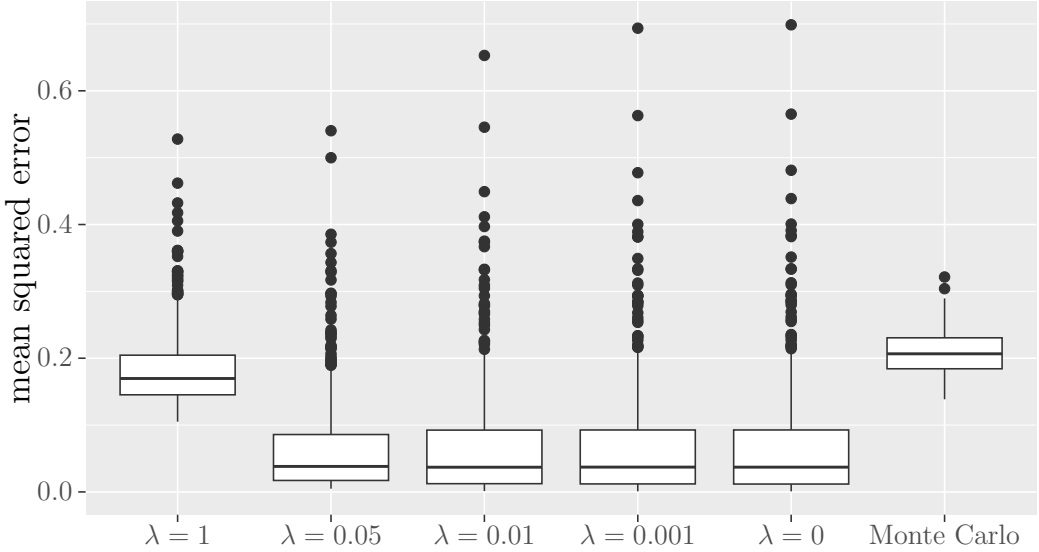


Figure 4: Mean squared error in the Black-Scholes model for the feature map setting based on 500 simulation runs for $N = 100\,000$ compared to Monte Carlo simulations (each with 1 000 samples) for 100 θ values chosen equidistant in $[0.1, 0.2]$.

In Theorem 2.9, we introduced feature maps. By choosing $\sigma = \tanh$, the MinMC setting for the Black-Scholes model can be applied here as well. Since the setting is not restricted to the interval $[0, 1]$ as in Example 2.6, we consider the volatility $\theta \in [0.1, 0.2]$ directly, without any rescaling. Analogous to Figure 2, we compare the mean squared error for different λ values based on 500 neural network fittings with Monte Carlo simulations in Figure 4. Here and in what follows, the mean squared error is computed on 100 equidistant points in the interval $[0.1, 0.2]$. We observe that the feature maps yield strong performance even for larger values of λ , indicating that regularization does not need to be significantly reduced. In all presented cases, MinMC provides better results than Monte Carlo simulations based on the same total number of random variables. In particular, the results for $\lambda \in \{0.05, 0.01, 0.001, 0\}$ are almost indistinguishable with the smallest median 0.0381 achieved for $\lambda = 0.05$. The medians, see Table 2, are slightly better than the optimal median of 0.0385 for $\lambda = 0$ in the previous simulations, see Table 1. The outliers of MinMC are similarly scattered in both settings, if we disregard the case $\lambda = 0.05$ in Figure 2.

As before, we compute a Monte Carlo average over M random variables for each model to obtain N training samples with the total number of random variables fixed at $M \cdot N = 120\,000$, see (7). The results for $\lambda = 0.01$ and $\lambda = 0.5$ are presented in Figure 5. In general, the mean squared error behaves similarly as in Figure 3: it decreases with increasing M , reaches a minimum, and subsequently increases as M becomes larger. However, the minimal me-

	median	25% quantile	75% quantile
$\lambda = 1$	0.1697	0.1453	0.2045
$\lambda = 0.05$	0.0381	0.0171	0.0858
$\lambda = 0.01$	0.0369	0.0123	0.0924
$\lambda = 0.001$	0.0371	0.0120	0.0927
$\lambda = 0$	0.0370	0.0118	0.0927
Monte Carlo	0.2066	0.1842	0.2305

Table 2: Median, 25% and 75% quantiles of the mean squared error obtained from 500 repeated price approximations for various λ values and the Monte Carlo method. These values correspond to the boxplots shown in Figure 4.

dians in Figure 5 are reached for significantly smaller values of M : 0.0535 at $M = 10$ for $\lambda = 0.5$ and 0.0095 at $M = 30$ for $\lambda = 0.01$. Although the optimal choice of M differs depending on the specific setting, the behavior of the mean squared error at its optimum remains consistent. Overall, MinMC clearly shows superior performance compared to a classical Monte Carlo simulation. This is particularly surprising since the Monte Carlo simulations are performed exactly on the 100 equidistant grid values in $[0, 1]$ on which both MinMC and the classical Monte Carlo are benchmarked against the Black-Scholes formula.

Now, we consider the Heston model in this setting of feature maps, see Example 2.9. We perform simulations under the Heston model in two different settings: in the first, we estimate the price function with respect to two parameters; in the second, with respect to three. In both cases, we fix the correlation at $\rho = -0.5$ and estimate the option price as a function of the mean reversion rate $\kappa \in [1, 10]$ and the long-term variance $\theta \in [0.2, 1]$. In the two-parameter case, we fix the volatility of volatility at $\sigma = 0.2$, whereas in the three-parameter case, σ varies within the range $[0.2, 0.5]$. In Figure 6 we visualize the price estimate by MinMC for $\lambda = 0.001$ based on a sample with $N = 600\,000$ random variables and maturity $T = 1/12$ in the two-parameter case.

In contrast to the Black-Scholes model, the Heston model does not admit a closed-form solution for option prices in the general case. Consequently, to compute a benchmark for evaluating the mean squared error, we approximate the price using Monte Carlo simulation. In the two-parameter setting, we discretize each parameter interval into 100 equidistant points, yielding a grid of 100^2 parameter combinations. For each grid point, we estimate the benchmark price using 10^6 Monte Carlo simulations. In the three-parameter case, we use 35 equidistant points per dimension, resulting in 35^3 total grid points, with the same number 10^6 of Monte Carlo simulations per point. The mean-squared errors in the following are calculated based on these benchmarks and grids depending on the case (2 or 3 parameters).

As in the Black-Scholes model, we perform pre-averaging using M Monte Carlo simulations per parameter Θ_i to determine our N random variables for the neural network fitting, see (7). We fix the total number of random variables to

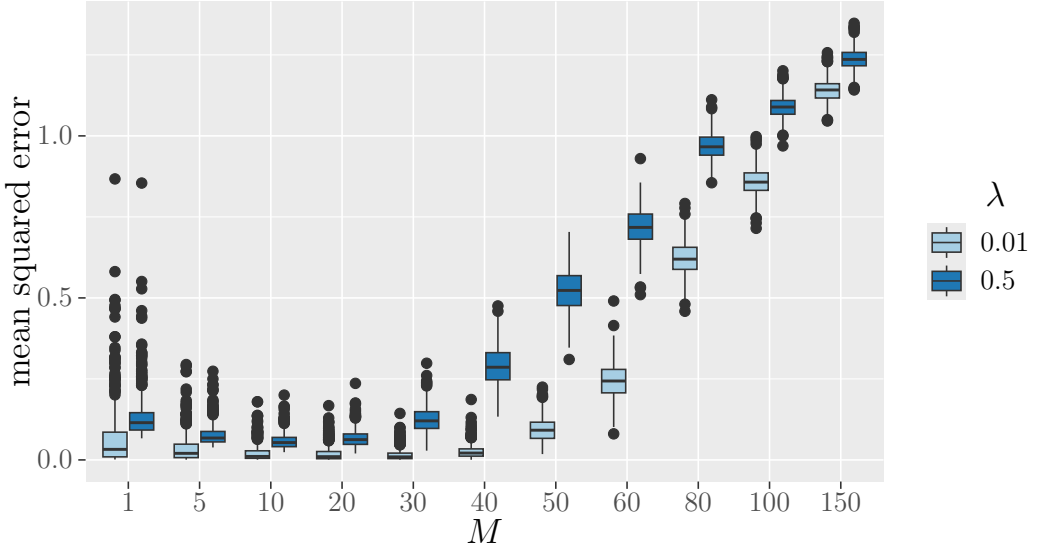


Figure 5: Mean squared error in the Black-Scholes model for the feature map setting based on 500 simulation runs for $\lambda = 0.01$ and $\lambda = 0.001$ with fixed number of random variables $M \cdot N = 120\,000$. For fixed M the simulations are based on the same samples.

$M \cdot N = 120\,000$ or $M \cdot N = 600\,000$, respectively. The neural network is then trained 500 times using different training sets in each run. For each trained model, we compute the corresponding price approximations and evaluate the mean squared error using the described benchmarks. The corresponding box-plots for different maturities are presented in Figures 7 and 8.

The first observation across all constellations is that the smaller the maturity, the smaller the mean squared error. Furthermore, for the same number of random variables, the case in which the function depends on two parameters is estimated more accurately than the case with three parameters. This is expected, as increasing the number of parameters complicates the approximation of the pricing function. This difference is particularly pronounced for $M \cdot N = 120\,000$, see Figure 7, but becomes significantly smaller for $M \cdot N = 600\,000$ in Figure 8, where the overall error levels are notably lower. Perhaps in the first case, the total number of random variables is too small to estimate a function in three variables. In Figure 7, the smallest median values are attained at $M = 5$, although they are comparable to those observed for $M \in \{1, 10\}$, where the boxplots indicate lower variability. A similar observation can be made for Figure 8, where, however, the best median is achieved at $M = 50$. Overall, the mean squared error in both figures behaves similar for the first three presented M values and then increases monotonically. Both figures suggest that having a greater number of grid points is more beneficial than using highly accurate grid points. A small value of M may lead to some improvement. This is likely due to the fact that the function depends

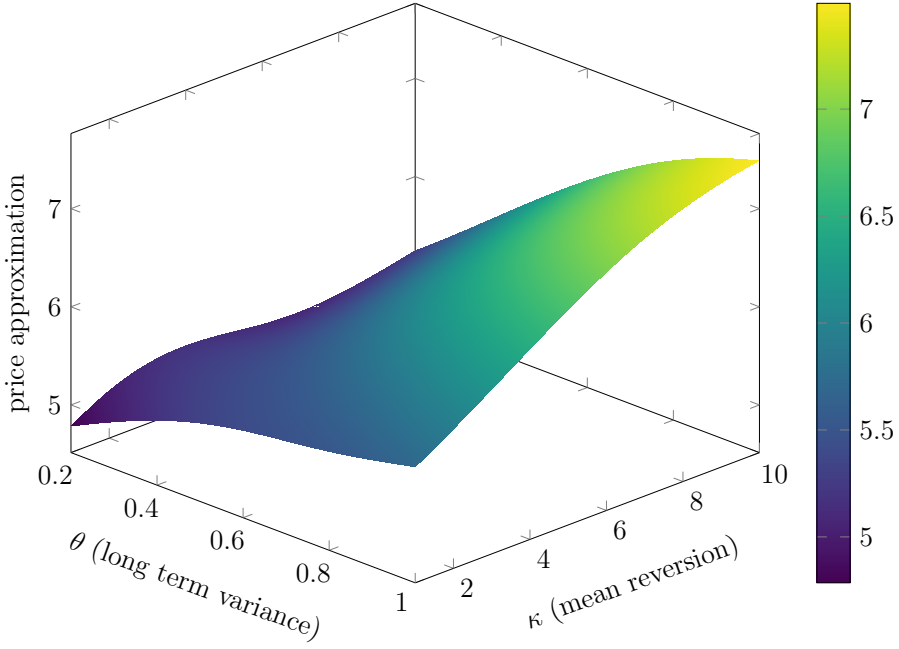


Figure 6: Heat map to visualize the MinMC approximation for a European call option price in the Heston model with $N = 600\,000$ random variables, correlation $\rho = -0.5$ and volatility of volatility $\sigma = 0.2$.

on multiple parameters. When $M \cdot N$ is too small, the function must first be explored across all relevant dimensions before more accurate evaluations contribute effectively to the estimation. Overall, also in this example, MinMC shows a strong performance gain compared to a classical Monte Carlo method.

A Operator theoretic results

In this section we provide all the results used from operator theory. We assume the same setting as in Section 2 and 3.

Lemma A.1. Let $C := \int_{\Gamma} (k(\theta, \theta))^2 \mu(d\theta) < \infty$ and $h \in H$. Then, we have

$$\mathbb{E}[h(\Theta)^4] \leq \|h\|^4 C < \infty.$$

Proof. Using the Cauchy-Schwarz inequality and the definition of the kernel yield $|h(\Theta)| = |\langle h, k_{\Theta} \rangle| \leq \|h\| \cdot \|k_{\Theta}\| = \|h\| \sqrt{k(\Theta, \Theta)}$. Thus, we get

$$\mathbb{E}[h(\Theta)^4] \leq \|h\|^4 \mathbb{E}[(k(\Theta, \Theta))^2] = \|h\|^4 C$$

where the last equality follows from $\mathbb{P}^{\Theta} = \mu$. \square

Lemma A.2. Let $h, g \in H$ with $h = g$ \mathbb{P}^{Θ} -a.s. Then, $h = g$.

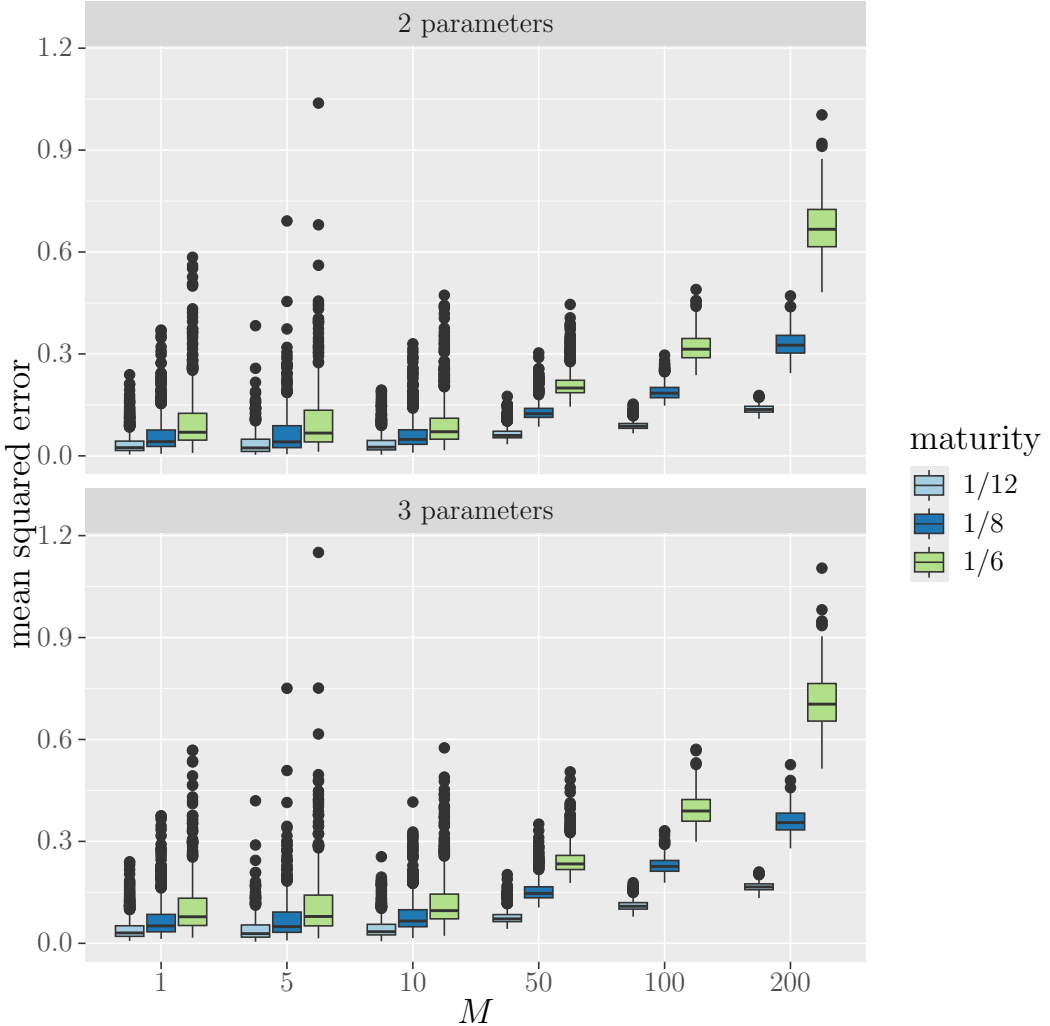


Figure 7: Mean squared error in the Heston model based on 500 simulation runs for various maturities with fixed number of random variables $M \cdot N = 120\,000$. For fixed M the simulations are based on the same samples.

Proof. Define $A := \{\gamma \in \Gamma : h(\gamma) = g(\gamma)\}$. By assumption, we find $\mathbb{P}(\Theta \in A) = \mathbb{P}^\Theta(A) = 1$. Since h, g are continuous, A is closed. Assumption (A2) and $\mathbb{P}^\Theta = \mu$ imply $A = \Gamma$, that is, $h = g$. \square

Lemma A.3. Let $\tilde{Q} \in L(H)$ be positive semidefinite, trace-class. Then, $\tilde{Q} + \lambda$ is invertible for any $\lambda > 0$ and $(\tilde{Q} + \lambda)^{-1}$ has operator norm at most λ^{-1} .

Proof. Since \tilde{Q} is positive semidefinite with spectral values $\lambda_i \geq 0$, the operator $\tilde{Q} + \lambda$ is positive definite with spectral values $\lambda_i + \lambda > 0$. Hence, $\tilde{Q} + \lambda$ is invertible and due to spectral mapping theorem [Pal94, 2.1.10 Theorem] its inverse has spectral values $(\lambda_i + \lambda)^{-1}$. Since the operator is self-adjoint and positive definite, the operator norm equals the supremum of the absolute values

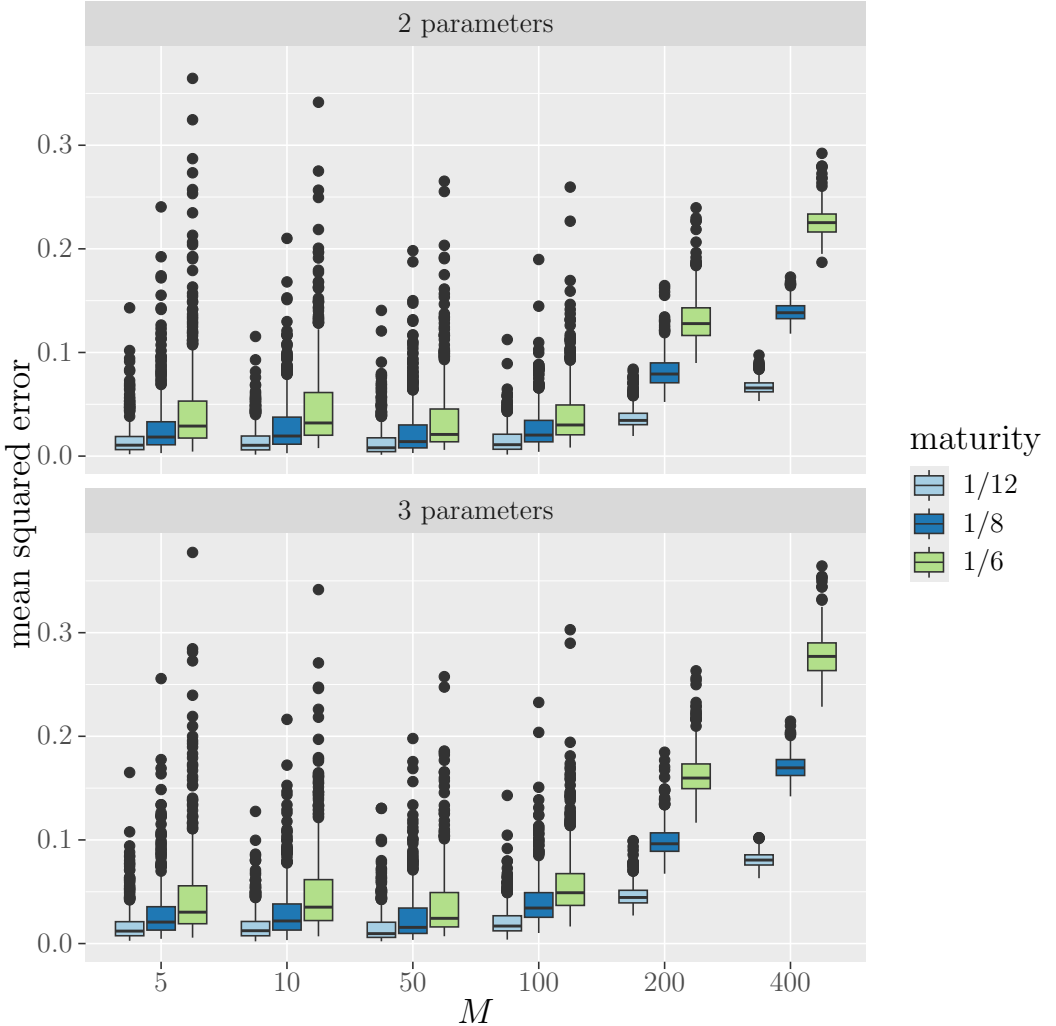


Figure 8: Mean squared error in the Heston model based on 500 simulation runs for various maturities with fixed number of random variables $M \cdot N = 600\,000$. For fixed M the simulations are based on the same samples.

of the spectral values which is bounded by λ^{-1} , see [Rud91, 10.13 Theorem (b), 12.31 Theorem (a)]. \square

Lemma A.4. Let $\tilde{Q} \in L(H)$ be positive semidefinite, trace-class, and let $\Pi : H \rightarrow H$ denote the orthonormal projector on the kernel of \tilde{Q} . Then, $\lambda(\tilde{Q} + \lambda)^{-1}$ converges to Π strongly as $\lambda \searrow 0$, i.e., for every $h \in H$ we have

$$\lim_{\lambda > 0, \lambda \rightarrow 0} \lambda(\tilde{Q} + \lambda)^{-1}h = \Pi h.$$

Moreover, if the kernel of \tilde{Q} is trivial, then

$$\lim_{\lambda > 0, \lambda \rightarrow 0} \lambda(\tilde{Q} + \lambda)^{-1}h = \mathbf{0}.$$

Proof. There exists an orthonormal basis $(e_i)_{i \in I}$ for some index set I such that e_i is an eigenvector of \tilde{Q} with some eigenvalue $\rho_i \geq 0$ for any $i \in I$ [DS88, p. 905, 4 Theorem]. We find that

$$\begin{aligned}\lambda(\tilde{Q} + \lambda)^{-1}h &= \sum_{i \in I} \langle h, e_i \rangle \lambda(\tilde{Q} + \lambda)^{-1}e_i \\ &= \sum_{i \in I} \langle h, e_i \rangle \lambda(\rho_i + \lambda)^{-1}e_i.\end{aligned}$$

Note that the following applies for each summand

$$\lim_{\lambda > 0, \lambda \rightarrow 0} \lambda(\rho_i + \lambda)^{-1}e_i = \Pi e_i = \begin{cases} 0 & \rho_i > 0, \\ e_i & \rho_i = 0, \end{cases}$$

with $\|\lambda(\rho_i + \lambda)^{-1}e_i\| \leq 1$. Consequently, we get

$$\lim_{\lambda > 0, \lambda \rightarrow 0} \sum_{i \in I} \langle h, e_i \rangle \lambda(\rho_i + \lambda)^{-1}e_i = \sum_{i \in I} \langle h, e_i \rangle \Pi e_i = \Pi h.$$

□

Lemma A.5. Let $\tilde{Q} \in L(H)$ be positive semidefinite, $\lambda > 0$, $\tilde{a} \in H$ and $c \in \mathbb{R}$. Then,

$$\tilde{V} : H \rightarrow \mathbb{R}, \quad \tilde{V}(h) := \langle \tilde{Q}h, h \rangle - 2\langle \tilde{a}, h \rangle + c + \lambda\|h\|^2$$

has a unique minimizer given by

$$\tilde{h}_0 := (\tilde{Q} + \lambda)^{-1}\tilde{a}$$

with objective value

$$\tilde{V}(\tilde{h}_0) = c - \langle \tilde{a}, \tilde{h}_0 \rangle.$$

Proof. \tilde{V} is convex and continuously differentiable. Consequently, $h \in H$ is a minimizer for \tilde{V} if and only if $\nabla \tilde{V}(h) = \mathbf{0}$. Since $\nabla \tilde{V}(h) = 2(\tilde{Q} + \lambda)h - 2\tilde{a}$ we find that $h \in H$ is a minimizer if and only if $(\tilde{Q} + \lambda)h = \tilde{a}$. Theorem A.3 yields invertibility of $\tilde{Q} + \lambda$ and, thus, that the claimed element is the minimizer. Moreover, inserting the minimizer \tilde{h}_0 into \tilde{V} implies the last equality. □

Lemma A.6. Let $\tilde{Q}_1, \tilde{Q}_2 \in L(H)$ be positive semidefinite and $\lambda > 0$. Then, we have

$$\|(\tilde{Q}_1 + \lambda)^{-1} - (\tilde{Q}_2 + \lambda)^{-1}\|_{\text{op}} \leq \frac{\|\tilde{Q}_1 - \tilde{Q}_2\|_{\text{op}}}{\lambda^2}.$$

Proof. For $D := \tilde{Q}_2 - \tilde{Q}_1$ we derive

$$\begin{aligned}(\tilde{Q}_1 + \lambda)^{-1} - (\tilde{Q}_2 + \lambda)^{-1} &= (\tilde{Q}_1 + \lambda)^{-1} \left(1 - (\tilde{Q}_1 + \lambda)(\tilde{Q}_1 + D + \lambda)^{-1} \right) \\ &= (\tilde{Q}_1 + \lambda)^{-1} D (\tilde{Q}_2 + \lambda)^{-1}.\end{aligned}$$

Lemma A.3 yields the claim. □

Lemma A.7. Let $h \in H$. Then, $h \otimes h$ is positive semidefinite, trace-class and Hilbert Schmidt. We also have

$$\|h \otimes h\|_{\text{op}} = \text{Tr}(h \otimes h) = \|h \otimes h\|_{HS} = \|h\|^2.$$

Proof. If $h = 0$, then the equality is trivial. Thus, we may assume that $h \neq 0$.

There is an orthonormal basis $(b_n)_{n \in \mathbb{N}}$ such that $b_1 := \frac{h}{\|h\|}$. We find that

$$\text{Tr}(h \otimes h) = \sum_{n \in \mathbb{N}} \langle (h \otimes h)b_n, b_n \rangle = \sum_{n \in \mathbb{N}} \langle h, b_n \rangle^2 = \langle h, b_1 \rangle^2 = \|h\|^2.$$

Since $(h \otimes h)^* = h \otimes h$ we get

$$\|h \otimes h\|_{HS}^2 = \text{Tr}(\|h\|^2(h \otimes h)) = \|h\|^4$$

and, hence,

$$\|h \otimes h\|_{HS} = \|h\|^2.$$

For the last equality, we have

$$\|h \otimes h\|_{\text{op}} \leq \|h\|^2$$

and

$$\|h \otimes h\|_{\text{op}} \geq \|(h \otimes h)b_1\| = \|h\|^2$$

as required. \square

Lemma A.8. The random operators $Q_N := \frac{1}{N} \sum_{k=1}^N k_{\Theta_k} \otimes k_{\Theta_k}$ for $N \in \mathbb{N}$ and the operator $Q := \mathbb{E}[k_{\Theta} \otimes k_{\Theta}] = \mathbb{E}[Q_1]$ are positive semidefinite, trace-class and Hilbert Schmidt. Moreover, $\text{Tr}(Q)$, $\|Q\|_{\text{op}}$, $\|Q\|_{HS}$ are all bounded by $\mathbb{E}[\|k_{\Theta}\|^2]$. If $f, g \in H$, then

$$\langle Qf, g \rangle = \mathbb{E}[f(\Theta)g(\Theta)] = \langle f, g \rangle_{\mathcal{L}^2(\mu)}.$$

Furthermore, if the support of μ is Γ , then Q is positive definite.

Proof. Q_N has obviously all the given properties. Note that

$$\|Q\|_{\text{op}} \leq \mathbb{E}[\|k_{\Theta}\|^2] < \infty$$

which shows that Q is well defined and positive semidefinite. We also know

$$\text{Tr}(Q_1) = \|k_{\Theta}\|^2$$

and, consequently, we find

$$\text{Tr}(Q) = \mathbb{E}[\|k_{\Theta}\|^2] < \infty$$

which yields that Q is trace-class and, hence, Hilbert Schmidt. Recall that for a positive semidefinite operator Q which is trace-class, we get the following inequality

$$\|Q\|_{HS}^2 \leq \|Q\|_{\text{op}} \text{Tr}(Q)$$

and, thus, we obtained the stated upper bound for the trace-norm, the operator norm and the Hilbert Schmidt norm of Q .

Now, assume that the support of μ is Γ and let $h \in H$ with $Qh = \mathbf{0}$. We have

$$0 = \langle Qh, h \rangle = \mathbb{E}[h(\Theta)^2].$$

Consequently, $h(\Theta) = \mathbf{0}$ \mathbb{P}^Θ -a.s. Since the support of $\mu = \mathbb{P}^\Theta$ is Γ we see that $h = \mathbf{0}$ on a dense set. Theorem A.2 implies $h = \mathbf{0}$ and hence the kernel of Q is trivial. \square

Lemma A.9. Let $\lambda \geq 0$ and define $f(x) := \frac{\lambda\sqrt{x}}{\lambda+x}$ for any $x \geq 0$. Then,

$$f(x) \leq \sqrt{\lambda}/2$$

for any $x \geq 0$.

Proof. Due to $f(0) = 0 \leq \sqrt{\lambda}/2$, we may assume $x > 0$. Note that $0 < \sqrt{x\lambda} \leq (x + \lambda)/2$ and, thus, we receive

$$f(x) \leq \sqrt{\lambda}/2$$

as required. \square

Proposition A.10. Let $\tilde{Q} \in L(H)$ be positive semidefinite. We define the semi-norm $\|f\|_{\tilde{Q}} := \|\tilde{Q}^{1/2}f\|$ for any $f \in H$. Then, for any $\lambda > 0$, $h \in H$ we get

$$\|\lambda(\tilde{Q} + \lambda)^{-1}h\|_{\tilde{Q}} \leq \sqrt{\lambda}\|h\|/2.$$

Furthermore, if $\tilde{Q} := Q$ is the operator from Lemma A.8, then for any $\lambda > 0$, $h \in H$ we have

$$\|\lambda(Q + \lambda)^{-1}h\|_{\mathcal{L}^2(\mu)} \leq \sqrt{\lambda}\|h\|/2.$$

Proof. We consider $f(x) := \frac{\lambda\sqrt{x}}{x+\lambda}$ and

$$f(\tilde{Q}) := \lambda\tilde{Q}^{1/2}(\tilde{Q} + \lambda)^{-1}.$$

Lemma A.9 yields $f(x) \leq \sqrt{\lambda}/2$ for any $x \geq 0$. The spectral mapping theorem implies that $f(\tilde{Q})$ is bounded linearly with

$$\|f(\tilde{Q})\|_{L(H)} \leq \sup \{|f(x)| : 0 \leq x \leq \|\tilde{Q}\|_{L(H)}\} \leq \sqrt{\lambda}/2.$$

We find

$$\begin{aligned}\|\lambda(\tilde{Q} + \lambda)^{-1}h\|_{\tilde{Q}} &= \|\lambda\tilde{Q}^{1/2}(\tilde{Q} + \lambda)^{-1}h\| \\ &\leq \|f(\tilde{Q})\|_{L(H)}\|h\| \\ &\leq \sqrt{\lambda}\|h\|/2\end{aligned}$$

which shows the first displayed inequality.

Now, let \tilde{Q} be the operator from Lemma A.8, i.e., $\tilde{Q} := Q = \mathbb{E}[k_\Theta \otimes k_\Theta]$. Then, we have $\langle Qf, g \rangle = \mathbb{E}[f(\Theta)g(\Theta)]$ for any $f, g \in H$. For $f \in H$ we compute

$$\begin{aligned}\|f\|_{\mathcal{L}^2(\mu)}^2 &= \mathbb{E}[f(\Theta)^2] \\ &= \langle Qf, f \rangle \\ &= \langle Q^{1/2}f, Q^{1/2}f \rangle \\ &= \|f\|_Q^2\end{aligned}$$

and the inequality results from the first part. \square

The following proposition shows that under some condition the optimizer for a non-degenerate regression problem, if exists, is obtained as the limit of the optimizers for the problem with an additional ridge term.

Proposition A.11. Let $\tilde{Q} \in L(H)$ be positive definite and trace-class, $\tilde{a} \in H$ and $c \in \mathbb{R}$. Assume that $\tilde{h}_0 \in H$ is a minimizer of

$$\tilde{V} : H \rightarrow \mathbb{R}, \quad \tilde{V}(h) := \langle \tilde{Q}h, h \rangle - 2\langle \tilde{a}, h \rangle + c.$$

and \tilde{h}_λ is the minimizer of $\tilde{V}_\lambda(h) := \tilde{V}(h) + \lambda\|h\|^2$ for any $\lambda > 0$ as given in Lemma A.5. Then,

$$\lim_{\lambda > 0, \lambda \rightarrow 0} \tilde{h}_\lambda = \tilde{h}_0.$$

Furthermore, if \tilde{Q} is the operator from Lemma A.8, we have

$$\|\tilde{h}_\lambda - \tilde{h}_0\|_{\mathcal{L}^2(\mu)} \leq \sqrt{\lambda}\|\tilde{h}_0\|/2.$$

Proof. Lemma A.5 yields that $\tilde{h}_\lambda = (\tilde{Q} + \lambda)^{-1}\tilde{a}$ for any $\lambda > 0$. Since \tilde{h}_0 is a minimizer for \tilde{V} we find that

$$\nabla \tilde{V}(\tilde{h}_0) = \mathbf{0}.$$

Due to $\nabla \tilde{V}(h) = 2(\tilde{Q}h - \tilde{a})$ for any $h \in H$ we see that $\tilde{Q}\tilde{h}_0 = \tilde{a}$. Note that $(\tilde{Q} + \lambda)^{-1}\tilde{Q} = 1 - \lambda(\tilde{Q} + \lambda)^{-1}$. For $\lambda > 0$ we calculate

$$\begin{aligned}\tilde{h}_\lambda &= (\tilde{Q} + \lambda)^{-1}\tilde{Q}\tilde{h}_0, \\ &= \tilde{h}_0 - \lambda(\tilde{Q} + \lambda)^{-1}\tilde{h}_0.\end{aligned}$$

Theorem A.4 implies

$$\lim_{\lambda > 0, \lambda \rightarrow 0} \tilde{h}_\lambda = \tilde{h}_0.$$

The bound on $\|\tilde{h}_\lambda - \tilde{h}_0\|_{\mathcal{L}^2(\mu)} = \|\lambda(\tilde{Q} + \lambda)^{-1}\tilde{h}_0\|_{\mathcal{L}^2(\mu)}$ is given in Proposition A.10. \square

The $\mathcal{L}^2(\mu)$ -norm and the RKHS norm have a relation, namely $\tilde{Q}^{1/2}$ is an isometry:

Lemma A.12. Let $\tilde{Q}^{1/2}$ be the positive semidefinite square root of $\tilde{Q} \in L(H)$. Then, we have for any $h \in H$ that $h \in \mathcal{L}^2(\mu)$ and

$$\|h\|_{\mathcal{L}^2(\mu)} = \|\tilde{Q}^{1/2}h\|.$$

Proof. Let $h \in H$. We find that

$$\int_{\Gamma} h(\theta)^2 \mu(d\theta) = \mathbb{E}[h(\Theta)^2] = \langle \tilde{Q}h, h \rangle = \|\tilde{Q}^{1/2}h\|^2 \leq \|\tilde{Q}^{1/2}\|_{\text{op}}^2 \|h\|^2 < \infty.$$

Consequently, we find $h \in \mathcal{L}^2(\mu)$ and

$$\|h\|_{\mathcal{L}^2(\mu)} = \|\tilde{Q}^{1/2}h\|_H.$$

\square

B Monte Carlo on a Hilbert space

Lemma B.1. Let $(b_n)_{n \in \mathbb{N}}$ be identical distributed, square-integrable and uncorrelated random variables on a Hilbert space. We have

$$\mathbb{E}\left[\left\|\frac{1}{N} \sum_{n=1}^N b_n - \mu\right\|^2\right] = \frac{\mathbb{E}[\|b_1 - \mu\|^2]}{N}$$

with $\mu := \mathbb{E}[b_1]$.

Proof. We derive

$$\left\|\frac{1}{N} \sum_{n=1}^N b_n - \mu\right\|^2 = \frac{1}{N^2} \sum_{n=1}^N \|b_n - \mu\|^2 + \frac{1}{N^2} \sum_{\substack{k,l=1 \\ k \neq l}}^N \langle b_k - \mu, b_l - \mu \rangle.$$

Taking expectation and using that the double-sum has zero expectation yields

$$\mathbb{E}\left[\left\|\frac{1}{N} \sum_{n=1}^N b_n - \mu\right\|^2\right] = \frac{\mathbb{E}[\|b_1 - \mu\|^2]}{N}$$

as required. \square

In the following, we denote by $L_{HS}(H)$ the Hilbert Schmidt operators, see [DS88, Section XI.6. Hilbert-Schmidt Operators].

Corollary B.2. Let $(B_n)_{n \in \mathbb{N}}$ be identical distributed, square-integrable and uncorrelated $L_{HS}(H)$ -valued random variables with $\mathbb{E}[\|B_1\|_{HS}^2] < \infty$. We have

$$\mathbb{E}\left[\left\|\frac{1}{N} \sum_{n=1}^N B_n - \mu\right\|_{HS}^2\right] = \frac{\mathbb{E}[\|B_1 - \mu\|_{HS}^2]}{N}$$

with $\mu := \mathbb{E}[B_1]$.

Proof. The set of Hilbert Schmidt operators $L_{HS}(H)$ with the Hilbert-Schmidt norm $\|\cdot\|_{HS}$ is a Hilbert space, see [DS88, p. 1011, 4 Theorem]. The corresponding scalar product is $\langle A, C \rangle_{HS} = \text{Tr}(AC^*)$. Consequently, Lemma B.1 can be applied to the sequence $(B_n)_{n \in \mathbb{N}}$ on this Hilbert space. \square

Acknowledgment

Computational support from the Zentrum für Informations- und Medientechnologie (ZIM) at Heinrich Heine University is gratefully acknowledged.

References

- [AF03] Robert A. Adams and John J. F. Fournier. *Sobolev Spaces*. Pure and Applied Mathematics. Academic Press, 2nd edition, 2003.
- [Aro50] Nachman Aronszajn. Theory of Reproducing Kernels. *Transactions of the American Mathematical Society*, 68(3):337–404, 1950.
- [BBG⁺21] Christian Beck, Sebastian Becker, Philipp Grohs, Nor Jaafari, and Arnulf Jentzen. Solving the kolmogorov pde by means of deep learning. *Journal of Scientific Computing*, 88(3), July 2021.
- [BC24] Cyril Bénézet and Stéphane Crépey. Handling model risk with xvas. *Frontiers of Mathematical Finance*, 3:490–519, 01 2024.
- [BDG24] Fred Espen Benth, Nils Detering, and Luca Galimberti. Pricing options on flow forwards by neural networks in a hilbert space. *Finance and Stochastics*, 28(1):81–121, 2024.
- [BS73] Fischer Black and Myron Scholes. The Pricing of Options and Corporate Liabilities. *Journal of Political Economy*, 81(3):637–654, 1973.

- [Con04] Rama Cont. Model uncertainty and its impact on the pricing of derivative instruments. *Mathematical Finance*, 16, 07 2004.
- [DP16] Nils Detering and Natalie Packham. Model risk of contingent claims. *Quantitative Finance*, 16(9):1357–1374, 2016.
- [DP21] Paul Dommel and Alois Pichler. Uniform function estimators in reproducing kernel hilbert spaces, 2021.
- [DS88] Nelson Dunford and Jakob T. Schwartz. *Linear Operators, Part 2: Spectral Theory, Self Adjoint Operators in Hilbert Space*. Wiley Classics Library. Wiley, 1988.
- [DS98] Norman R. Draper and Harry Smith. *Applied Regression Analysis*. John Wiley & Sons, New York, NY, 3rd edition, 1998.
- [Fil01] Damir Filipović. *Consistency Problems for Heath–Jarrow–Morton Interest Rate Models*. Springer Science & Business Media, 2001.
- [FPP22] Magnus Grønnegaard Frandsen, Tobias Cramer Pedersen, and Rolf Poulsen. Delta force: option pricing with differential machine learning. *Digital Finance*, 4(1):1–15, 2022.
- [FPY22] Damir Filipović, Markus Pelger, and Ye Ye. Stripping the discount curve — a robust machine learning approach. *Forthcoming, Management Science*, 2022.
- [FS25] Damir Filipović and Paul Schneider. Joint estimation of conditional mean and covariance for unbalanced panels, 2025.
- [Gla04] Paul Glasserman. *Monte Carlo methods in financial engineering*. Springer, New York, 2004.
- [Här90] Wolfgang Härdle. *Applied Nonparametric Regression*. Cambridge University Press, Cambridge, UK, 1990.
- [HM85] Wolfgang Härdle and James S. Marron. Optimal bandwidth selection in nonparametric regression function estimation. *The Annals of Statistics*, 13(4):1465–1481, 1985.
- [HS20] Brian Huge and Antoine Savine. Differential machine learning: The shape of things to come. *Risk*, pages 76–81, 2020.
- [HSW89] Kurt Hornik, Maxwell Stinchcombe, and Halbert White. Multi-layer feedforward networks are universal approximators. *Neural Networks*, 2(5):359–366, 1989.
- [Jon15] Jonathan H.Manton and Pierre-Olivier Amblard. *A Primer on Reproducing Kernel Hilbert Spaces*, volume 8. Foundations and Trends® in Signal Processing, 2015.

- [JS20] Valeriane Jokhadze and Wolfgang M. Schmidt. Measuring model risk in financial risk management and pricing. *International Journal of Theoretical and Applied Finance*, 23(02):2050012, 2020.
- [LQT24] Emese Lazar, Shuyuan Qi, and Radu Tunaru. Measures of model risk for continuous-time finance models. *Journal of Financial Econometrics*, 22(5):1456–1481, 02 2024.
- [MPV12] Douglas C. Montgomery, Elizabeth A. Peck, and G. Geoffrey Vining. *Introduction to Linear Regression Analysis*. John Wiley & Sons, Hoboken, NJ, 5th edition, 2012.
- [Pag18] Gilles Pagès. *Numerical Probability: An Introduction with Applications to Finance*. Universitext. Springer Cham, 2018.
- [Pal94] Theodore W. Palmer. *Banach Algebras and the General Theory of *-Algebras*. Encyclopedia of Mathematics and its Applications. Cambridge University Press, 1994.
- [Rud91] Walter Rudin. *Functional Analysis*. International series in pure and applied mathematics. McGraw-Hill, 1991.
- [SFL11] Bharath K. Sriperumbudur, Kenji Fukumizu, and Gert R.G. Lanckriet. Universality, Characteristic Kernels and RKHS Embedding of Measures. *Journal of Machine Learning Research*, 12(70):2389–2410, 2011.
- [SHS01] Bernhard Schölkopf, Ralf Herbrich, and Alexander J. Smola. A generalized representer theorem. *Computational Learning Theory*, pages 416–426, 2001.
- [Sto77] Charles J. Stone. Consistent nonparametric regression. *The Annals of Statistics*, 5(4):595–620, 1977.
- [Sto80] Charles J. Stone. Optimal rates of convergence for nonparametric estimators. *The Annals of Statistics*, 8(6):1348–1360, 1980.